JGR Oceans

RESEARCH ARTICLE
10.1029/2024JC021178

Distinct Impacts of Increased Atlantic and Pacific Ocean Heat Transport on Arctic Ocean Warming and Sea Ice Decline

Kexin Cheng[1,2,3], Qi Shu[1,2,3,4,5], Qiang Wang[6], Zhenya Song[1,2,3], Yan He[1,2,3], Shizhu Wang[1,2,3], Rongrong Pan[1,2,3], Haibo Bi[7], and Fangli Qiao[1,2,3]

[1]First Institute of Oceanography and Key Laboratory of Marine Science and Numerical Modeling, Ministry of Natural Resources, Qingdao, China, [2]Laboratory for Regional Oceanography and Numerical Modeling, Qingdao Marine Science and Technology Center, Qingdao, China, [3]Shandong Key Laboratory of Marine Science and Numerical Modeling, Qingdao, China, [4]Shanghai Key Laboratory of Polar Life and Environment Sciences (Shanghai Jiao Tong University), Shanghai, China, [5]Key Laboratory of Polar Ecosystem and Climate Change (Shanghai Jiao Tong University), Ministry of Education, Shanghai, China, [6]Alfred Wegener Institute, Helmholtz Centre for Polar and Marine Research (AWI), Bremerhaven, Germany, [7]Key Laboratory of Ocean Observation and Forecasting and Key Laboratory of Ocean Circulation and Waves, Institute of Oceanology, Chinese Academy of Sciences, Qingdao, China

Abstract Increased ocean heat transport (OHT) to the Arctic Ocean from the Atlantic and Pacific oceans contributes to Arctic Ocean warming and sea ice decline in a warming climate, processes known as Atlantification and Pacification, respectively. However, the separate impacts of these OHTs and their magnitudes remain unclear. This study uses a fully coupled climate model (FIO-ESM v2.1) to investigate the specific impacts of increased Atlantic and Pacific OHTs on Arctic Ocean temperature, sea ice extent, and sea ice concentration. Our sensitivity experiments reveal that increased Atlantic OHT affects the temperature of the entire Arctic Ocean with the greatest impacts found in the Barents Sea and Eurasian Basin and at intermediate depths of the Arctic basin. The warming extent and efficiency from increased Atlantic OHT is considerably greater than that from Pacific OHT. Without warming of the Atlantic Water inflow, the rate of Arctic Ocean warming would decrease by approximately 50%. Increased Pacific OHT mainly affects the upper ocean in the Pacific sector, including the Chukchi Sea, East Siberian Sea, and Canada Basin. Increased OHT from both the Atlantic and Pacific oceans leads to notable sea ice decline with distinct regional and seasonal variations. Increased Atlantic OHT contributes to sea ice decline across most of the Arctic Ocean, particularly in the Barents Sea, the Kara Sea, and the central Arctic. In contrast, increased Pacific OHT leads to sea ice loss dominantly in the Pacific sector, including the Chukchi, the East Siberian, and the Beaufort seas.

Plain Language Summary Under climate change, the rate of Arctic Ocean warming is approximately two to three times that of the global ocean average, a phenomenon called "Arctic Ocean Amplification." Increase in ocean heat transport (OHT) from the Atlantic and Pacific oceans via the Arctic gateways is one of the key drivers for the amplified warming in the Arctic Ocean. However, the separate impacts of increased OHT from Atlantic and Pacific waters on Arctic Ocean warming remain unclear. This study investigates their separate effects on Arctic Ocean temperature and sea ice through numerical sensitivity experiments. The results indicate that the influence of increased Atlantic OHT is more pronounced and efficient than that of Pacific OHT. Although increased Pacific OHT mainly affects the Pacific sector, increased Atlantic OHT basically influences the entire Arctic Ocean, including both the Atlantic and the Pacific sectors. Increased Pacific OHT mainly increases the upper ocean temperature, whereas the impacts of increased Atlantic OHT are evident throughout the water column, with the most significant impacts occurring at intermediate depths.

Key Points:

- Warming effect of increased Atlantic ocean heat transport (OHT) would expand to the entire Arctic Ocean
- Without increased Atlantic OHT, the warming rate of the Arctic Ocean would be reduced by approximately 50%
- Atlantic OHT is diagnosed to affect sea ice across most of the Arctic Ocean, whereas Pacific OHT could affect sea ice in the Pacific sector

Supporting Information:

Supporting Information may be found in the online version of this article.

Correspondence to:

Q. Shu,
shuqi@fio.org.cn

Citation:

Cheng, K., Shu, Q., Wang, Q., Song, Z., He, Y., Wang, S., et al. (2025). Distinct impacts of increased Atlantic and Pacific Ocean heat transport on Arctic Ocean warming and sea ice decline. *Journal of Geophysical Research: Oceans*, *130*, e2024JC021178. https://doi.org/10.1029/2024JC021178

Received 7 APR 2024
Accepted 27 FEB 2025

Author Contributions:

Conceptualization: Qi Shu
Funding acquisition: Qi Shu
Investigation: Kexin Cheng
Methodology: Kexin Cheng, Qi Shu
Software: Kexin Cheng, Yan He
Validation: Kexin Cheng, Qi Shu, Qiang Wang
Visualization: Kexin Cheng, Qi Shu, Rongrong Pan
Writing – original draft: Kexin Cheng, Qi Shu
Writing – review & editing: Kexin Cheng, Qi Shu, Qiang Wang, Zhenya Song, Yan He, Shizhu Wang, Rongrong Pan, Haibo Bi, Fangli Qiao

1. Introduction

Notable changes in the climate of the Arctic have been detected by observations and simulations. Observations show rapid warming of the Arctic troposphere since the 1990s with the maximum warming rate near the surface in autumn and winter (Cohen et al., 2014, 2020; Wang & Overland, 2012). The rate of increase in near-surface air temperature in the Arctic is more than twice that of the global average (Cohen et al., 2014, 2020; Graversen et al., 2008; Rantanen et al., 2022; Wang & Overland, 2012), a phenomenon known as "Arctic Amplification." Climate model simulations indicate that the Arctic Ocean will also warm faster than the global ocean average in a

warming climate, which is a phenomenon called "Arctic Ocean Amplification" (Shu et al., 2022). Meanwhile, notable decline in Arctic sea ice has also been observed (Notz & Stroeve, 2016; Onarheim et al., 2018).

Previous studies indicated that increased ocean heat transport (OHT) to the Arctic plays a key role in Arctic Ocean warming and winter sea ice decline (Årthun et al., 2012; Carmack et al., 2015; Docquier & Koenigk, 2021; Dörr et al., 2021; Lien et al., 2017; Polyakov et al., 2020; Serreze et al., 2016; Woodgate, 2012). The increase in OHT by Atlantic Water and Pacific Water is considered an important reason for future rapid Arctic Ocean warming (Dörr et al., 2024; Shu et al., 2022). Moreover, OHT is an important driver of winter sea ice variability and long-term trends in the Barents Sea, Kara Sea, and southern Chukchi Sea, and the influence of OHT on sea ice is expected to expand toward the Laptev Sea and the central Arctic Ocean in the future (Dörr et al., 2021).

Recent strong ocean warming and sea ice loss has been witnessed in the Eurasian sector of the Arctic Ocean (Årthun et al., 2012; Barton et al., 2018; Polyakov et al., 2017), and it has been proposed that this Arctic Atlantification is mainly caused by the process of anomalous OHT from the North Atlantic to the Arctic Ocean (Årthun et al., 2012; Sandø et al., 2010). Arctic Atlantification is characterized by notable ocean warming, weakening in upper-ocean stratification, and winter sea ice decline in the Barents Sea, eastern Eurasian Basin, and the adjacent Kara and Greenland seas (Boitsov et al., 2012; Matishov et al., 2012; Polyakov et al., 2017; Schlichtholz, 2019; Skagseth et al., 2020; Smedsrud et al., 2013). The strong coupling of the climate system induces concurrent variations in heat, sea ice, salinity, and stratification within the Arctic, providing further evidence of Arctic Atlantification (Ingvaldsen et al., 2021).

Arctic Pacification, the counterpart to Atlantification associated with Pacific Water inflow through the Bering Strait, has also been observed, as evidenced by strengthened upper-ocean warming in the Canada Basin (Polyakov et al., 2020; Serreze et al., 2016; Woodgate, 2018). A distinct signature of climate change in the Pacific sector of the Arctic Ocean is the increase of both the influx and the warming of Pacific Water recorded by mooring observations in the Bering Strait since the 1990s (Woodgate, 2018). The increased Pacific Water heat flux through the Bering Strait has contributed to warming and sea ice loss in the Amerasian Basin (Shimada et al., 2006; Woodgate et al., 2010). A doubling of the heat flux from 2001 to 2007 was sufficient to explain one-third of the volume loss of Arctic sea ice in summer 2007 (Woodgate et al., 2010). Enhanced inflow of warm Pacific Water into the Amerasian Basin triggers a positive feedback mechanism (Shimada et al., 2006), whereby weaker sea ice becomes more susceptible to atmospheric wind forcing furthering wind-driven transport of Pacific Water off the shelf and into the central basin (Timmermans et al., 2014; Woodgate et al., 2010). A study based on in situ, satellite, and modeling data (Serreze et al., 2016) concluded that oceanic heat flux through the Bering Strait (in April–June) might explain 68% of the variance in the timing of sea ice retreat in the Chukchi Sea.

Climate model projections showed that the increase in OHT by Atlantic and Pacific waters will continue under global warming scenarios (Årthun et al., 2019; Polyakov et al., 2020; Shu et al., 2021), indicating future poleward expansion of Atlantification and Pacification in the Arctic Ocean. Dörr et al. (2021) report that the influence of Atlantic and Pacific ocean heat transports on winter sea ice would expand poleward into the Arctic Ocean in the future, and that their combined influence is anticipated to cover a large part of the Arctic Ocean by 2050–2079. The expanding impacts on sea ice could divide the Arctic Ocean into two regimes with Atlantic ocean heat transport mainly affecting sea ice in the Eurasian Arctic (west of the Laptev Sea) and Pacific ocean heat transport affecting sea ice in the Amerasian Arctic (Dörr et al., 2021, 2024; Muilwijk et al., 2023; Richards et al., 2022). However, the separate impacts of these OHTs and the magnitude of their regional influences on sea ice decline and especially on Arctic Ocean warming remain unclear.

In this study, we conducted numerical experiments using the First Institute of Oceanography-Earth System Model version 2.1 (FIO-ESM v2.1) to investigate the separate impacts of increased Atlantic OHT and Pacific OHT on Arctic Ocean warming and sea ice decline in a warming climate. The remainder of the paper is organized as follows. The model is introduced and the numerical experimental design is described in Section 2. Section 3 presents the results of the numerical experiments. Finally, a discussion and our conclusions are presented in Section 4.

Table 1
Numerical Experimental Design

Experiment name	Temperature nudging at the barents sea opening and fram strait	Temperature nudging at the bering strait	Motivation
CTRL	No	No	Standard simulations
BS_BSO_FS_nudging	Yes	Yes	To eliminate the increase of OHT from the Atlantic and Pacific waters
BSO_FS_nudging	Yes	No	To eliminate the increase of OHT from the Atlantic Water
BS_nudging	No	Yes	To eliminate the increase of OHT from the Pacific Water

2. Model Description and Numerical Experimental Design

2.1. Description of FIO-ESM v2.1

The model used in this study is FIO-ESM v2.1 (Shu et al., 2024), which is an updated version of FIO-ESM v2.0 (Bao et al., 2020) that participated in the Climate Model Intercomparison Project Phase 6 (CMIP6; Eyring et al., 2016). The updates include upgrading the sea ice component model from the Los Alamos Sea Ice Model (CICE) version 4.0 (CICE4.0) to CICE6.0 and improving the ice-ocean heat exchange process from a two-equation boundary condition parameterization to a more realistic three-equation boundary condition parameterization. Numerical experiments showed that the underestimation of Arctic summer sea ice extent (SIE) found in FIO-ESM v2.0 is substantially improved by the model enhancements (Shu et al., 2024).

FIO-ESM v2.1 consists of five model components: an atmospheric general circulation model (the Community Atmosphere Model version 5 (CAM5); Neale et al., 2012), a land surface model (the Community Land Model version 4.0 (CLM4); Lawrence et al., 2011), an ocean circulation model (the Parallel Ocean Program (POP2); Smith et al., 2010), an ocean surface wave model (the MASNUM surface wave model; Qiao et al., 2016), and a sea ice model (CICE6.0; Duvivier, 2018). All model components are coupled by the CPL7 coupler. The horizontal resolution of CAM5 and CLM4 is 1.25° longitude × 0.9° latitude, whereas that of POP2, MASNUM wave model, and CICE6.0 is approximately 1.1° longitude × 0.27°–0.54° latitude. The numbers of vertical layers in CAM5 and POP2 are 30 and 61, respectively. CAM5, CLM4, and CICE6.0 exchange data with the coupler every 30 min, whereas POP2 and MASNUM exchange data with the coupler at a 3-hr interval.

2.2. Numerical Experimental Design

Four numerical experiments were conducted using FIO-ESM v2.1 to investigate the distinct impacts of Atlantic OHT and Pacific OHT on the Arctic Ocean and Arctic sea ice (Table 1). The first experiment was a control experiment (CTRL) that consisted of a historical run from 1850 to 2014 and a Shared Socioeconomic Pathway 585 (SSP5-8.5) projection run from 2015 to 2100. The historical and projection runs followed the CMIP6 protocol. The SSP5-8.5 scenario is characterized by rapid and fossil-fueled development with high challenges to mitigation and low challenges to adaptation (Riahi et al., 2017). It represents the high end of the range of future pathways with effective radiative forcing of 8.5 W m^{-2} in 2100 (O'Neill et al., 2016). Compared with other relatively low-emission scenarios, the effects of increased OHT under SSP5-8.5 scenario are readily distinguishable from the natural variability.

We also designed and conducted three sensitivity experiments: BS_BSO_FS_nudging, BSO_FS_nudging, and BS_nudging (Table 1). Each sensitivity experiment also consisted of a historical run (1950–2014) and a SSP5-8.5 projection run (2015–2100); however, their historical runs comprised the branch runs from CTRL starting from 1950.

The increase in OHT through the Arctic Ocean gateways in a warming climate is mainly attributable to ocean temperature rather than to ocean velocity (Shu et al., 2022), and therefore, to largely eliminate the positive trends of OHT by Atlantic Water and Pacific Water, sea water temperature in both historical and projection runs in the sensitivity experiments at the corresponding Arctic Ocean gateways (Bering Strait, Fram Strait and Barents Sea Opening; Figure 1) was constrained to the monthly climatological mean of CTRL during 1921–1950, when the signs of climate change were not yet prominent. To constrain the simulations of temperature, a nudging method (Liu et al., 2019) was used. In the BS_BSO_FS_nudging experiment, ocean temperature was constrained at all the three gateways (Table 1). In the BSO_FS_nudging experiment, ocean temperature was constrained at the Barents

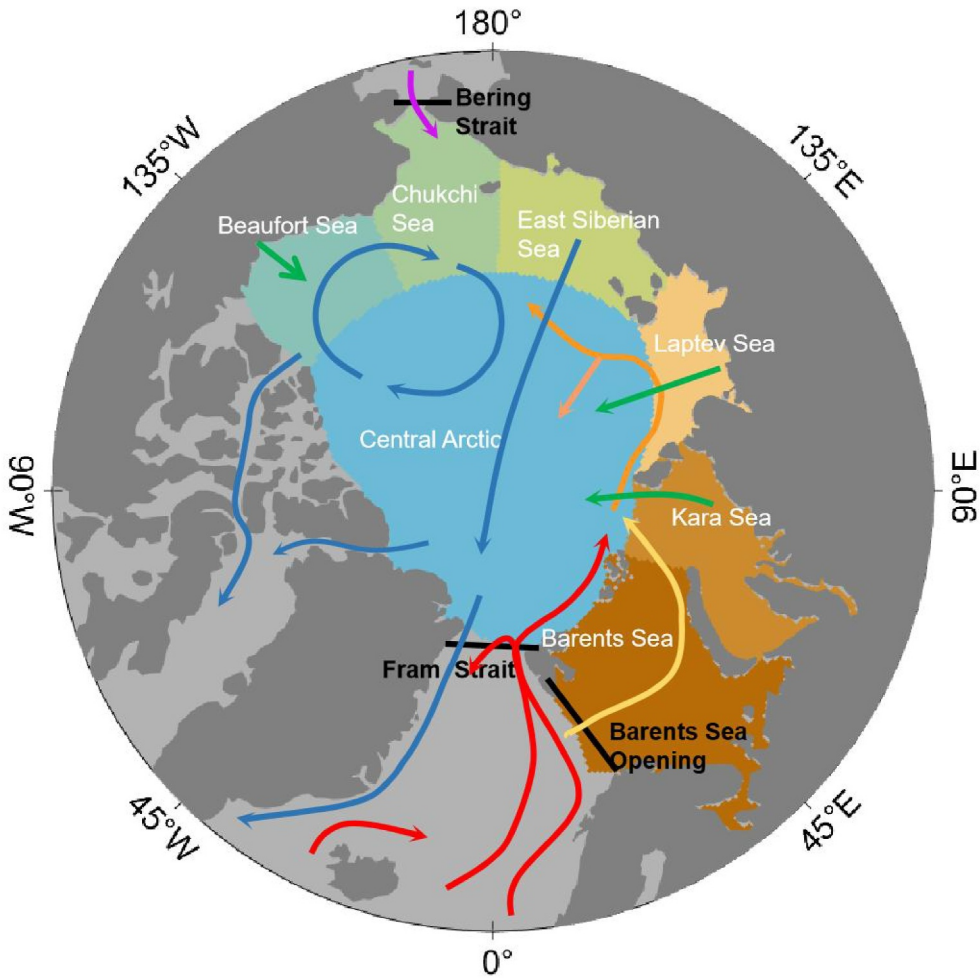

Figure 1. Schematic of the main ocean circulations in the pan-Arctic Ocean. Atlantic Water Barents Sea branch is indicated by yellow arrows, Fram Strait branch by red arrows, and orange arrows represent the two branches that join in the St. Anna Trough. Pacific Water inflow is shown by the magenta arrow. The circulation of freshwater originating from land is represented by green arrows, while the upper ocean circulation is depicted by blue arrows. Black lines indicate the gateways consisting of the Bering Strait, the Barents Sea Opening, and the Fram Strait. The Arctic Ocean in this study is defined as the ocean area to the north of the three gateways, which includes the central Arctic Ocean, the Barents Sea, the Kara Sea, the Laptev Sea, the East Siberian Sea, the Chukchi Sea, and the Beaufort Sea.

Sea Opening and Fram Strait. Finally, in the BS_nudging experiment, ocean temperature was constrained at the Bering Strait. The latitudinal bands for nudging near the Bering Strait and Fram Strait were taken as 63°N–66°N and 77°N–80°N, respectively. The longitudinal range for nudging at the Barents Sea Opening was set to 17° E−22°E. Within these areas, the ocean temperature in each model step was adjusted using the nudging method by applying the difference between the modeled temperature and the climatological temperature. The nudging timescale was set to one day, ensuring that the ocean temperature could stay near the climatological values of the period of 1921–1950.

Sensitivity experiments allowed us to investigate the impacts of increased Atlantic OHT by comparing the simulations between the BSO_FS_nudging and CTRL experiments and to investigate the impacts of increased Pacific OHT through comparison of the simulations of the BS_nudging and CTRL experiments. We also could investigate the combined impacts of increased Atlantic OHT and Pacific OHT through comparison of the simulations of the BS_BSO_FS_nudging and CTRL experiments.

Table 2
Ocean Volume Transport (Sv) and Heat Transport (TW) at the Barents Sea Opening, the Bering Strait, and the Fram Strait Based on Observations, Reanalysis Data Sets, and Simulations by FIO-ESM v2.1

		Bering strait	Barents sea opening	Fram Strait
Volume transport (Sv)	FIO-ESM v2.1	0.89	2.5	−1.4
		0.88		
	Observation	0.8[a]	~2.0[c]	−2.0[d]
		1.0[b]		
Heat transport (TW)	FIO-ESM v2.1	3.1	57.2	Atlantic Water: 20.7
			58.4	Net: 13.2
	Observation/reanalysis data sets	4.62[e]	48[f]	Atlantic Water: (26–50)[d]
			62[g]	Net: (6 − 42)[h]

[a]1990–2004 (Roach et al., 1995; Woodgate & Aagaard, 2005). [b]2003–2015 (Woodgate, 2018). [c]1997–2007 (Smedsrud et al., 2010, 2013). [d]1997–2006 (Schauer et al., 2008). [e]1991–2019 (Wang et al., 2023). [f]1997–2006 (Skagseth et al., 2008). [g]2002–2017 (Nguyen et al., 2021). [h]1993–2010 (Uotila et al., 2019).

2.3. Ocean Volume Transport and Ocean Heat Transport

The ocean volume transport (OVT) and OHT through each Arctic Ocean gateway were calculated using monthly potential temperature and ocean velocity as follows:

$$OVT = \int_{-H(\lambda)}^{0} \int_{\lambda_1(z)}^{\lambda_2(z)} v d\lambda dz \tag{1}$$

$$OHT = \rho_o C_p \int_{-H(\lambda)}^{0} \int_{\lambda_1(z)}^{\lambda_2(z)} v(\theta - \theta_{ref})\, d\lambda dz \tag{2}$$

where v is ocean velocity normal to the section of each gateway, θ is potential temperature, ρ_o is seawater density, C_p is the specific heat capacity at constant pressure of seawater, θ_{ref} is the reference temperature (set to 0°C), H is water depth, and λ is the distance along the gateway transect. In this study, the latitudinal positions of the Bering and Fram Straits are taken as 66°N and 80°N, respectively. The longitudinal position of the Barents Sea Opening is 20°E.

3. Results

3.1. Simulated Ocean Volume Transport, Ocean Heat Transport, and Arctic Ocean Warming

We first evaluated the simulated OVTs and OHTs through the three Arctic Ocean gateways in the CTRL experiment to validate the model. The values of OVT and OHT based on observations, reanalysis data sets, and the CTRL experiment are listed in Table 2. Net OVT through the Bering Strait based on observations are 0.8 ± 0.2 Sv during 1990–2004 (Roach et al., 1995; Woodgate & Aagaard, 2005) and 1.0 ± 0.05 Sv during 2003–2015 (Woodgate, 2018). The results of the CTRL experiment are 0.89 Sv during 1990–2014 and 0.88 Sv during 2003–2015 based on FIO-ESM v2.1, which are close to the observations. The net OVT through the Barents Sea Opening is approximately 2.0 Sv based on observations during 1997–2007 (Smedsrud et al., 2010, 2013). The result of the CTRL experiment is 2.5 Sv during 1997–2007 from FIO-ESMv2.1, representing a slight overestimation compared with the observations. The net OVT through Fram Strait is −2.0 ± 2.7 Sv based on observations during 1997–2006 (Schauer et al., 2008). The large deviation in the observations might reflect the fact that the OVT of both the inflow and the outflow through the Fram Strait are greatly variable. The result of the CTRL experiment is −1.4 Sv during 1997–2006, that is, within the range of observational uncertainty. Therefore, the climatology of the net OVT through the main Arctic Ocean gateways is well represented in CTRL.

Observations indicate that net OHT through the Bering Strait is 4.62 TW during 1991–2019 (Wang et al., 2023), whereas the result of the CTRL experiment is 3.1 TW during 1991–2019. Net OHT through the Barents Sea Opening is 48 TW during 1997–2006 based on the estimation by Skagseth et al. (2008) and 62 TW during 2002–

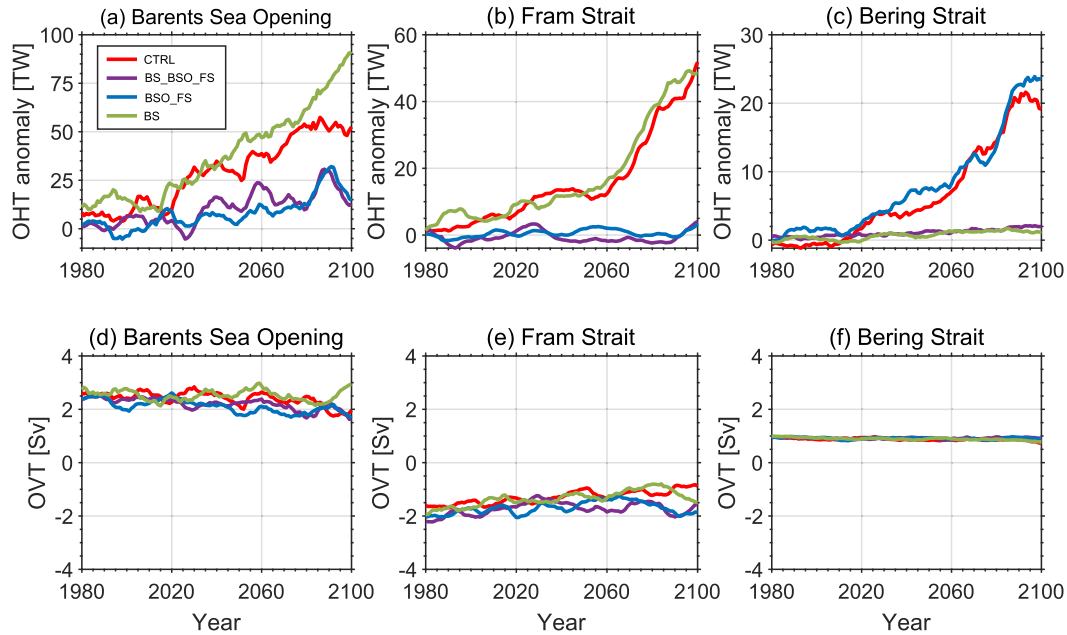

Figure 2. 11-year smoothed anomalies (relative to 1950–1979) of inflow ocean heat transport (OHT, a–c) and 11-year smoothed net ocean volume transport (OVT, (d–f)) through the Barents Sea Opening (a and d), Bering Strait (b and e), and Fram Strait (c and f). Red, purple, blue, and green lines represent the results of the CTRL, BS_BSO_FS_nudging, BSO_FS_nudging, and BS_nudging experiments, respectively.

2017 based on the estimation by Nguyen et al. (2021). The result of the CTRL experiment is 57.2 TW during 1997–2006 and 58.4 TW during 2002–2017. On the basis of the observational estimation by Schauer et al. (2008), OHT by Atlantic Water (warmer than 1°C) through the Fram Strait is between 26 and 50 TW during 1997–2006, whereas the result from the CTRL experiment is 20.7 TW during 1997–2006. Net OHT through the Fram Strait based on reanalysis data sets ranges between 6 and 42 TW, and it is 13.2 TW in the CTRL experiment during 1993–2010. Overall, the CTRL-simulated OHTs through the three main gateways are considered reasonable.

Figure 2 shows the inflow OHT anomalies and the net OVTs through the three gateways in the CTRL experiment and the three sensitivity experiments. The OHT increase at the Barents Sea Opening and the Fram Strait is relatively similar in CTRL and BS_nudging (Figures 2a and 2b), and the OHT increase at Bering Strait is relatively similar in CTRL and BSO_FS_nudging (Figure 2c). This indicates that the increase in OHT in the BS_nudging experiment is mostly driven by Atlantic OHT, whereas the Pacific OHT in the BSO_FS_nudging experiment mainly contributes to the increase in OHT. The net OVTs through the three gateways have no large trends (Figures 2d–2f), indicating that the increase in OHT is mainly due to sea water temperature warming rather than the increase of OVT, which is consistent with previous study (Shu et al., 2022).

We also compared full-depth-averaged Arctic Ocean warming in CTRL experiment with the results of CMIP6 multimodel mean (Table 3). 27 models from CMIP6 are used to calculate multimodel mean (Text S1 in Supporting Information S1). Table 3 shows that Arctic Ocean warming in CTRL experiment aligns well with the CMIP6 multi-model mean results, providing evidence for the reliability and validity of the FIO-ESM v2.1 results.

3.2. Impacts on the Arctic Ocean Warming

The time series of full-depth-averaged ocean temperature for each region of the Arctic Ocean are shown in Figure 3. The CTRL experiment projects an increase in Arctic Ocean temperature in the future. The Barents Sea is anticipated to experience the most rapid warming, with a temperature rise of approximately 5°C by the end of the century (Table 3). The East Siberian Sea and Kara Sea would both heat up by approximately 4°C, the Chukchi Sea and Laptev Sea would both be warming by approximately 2–3°C, the central Arctic Ocean would be heated by approximately 1.3°C, and the Beaufort Sea would have a temperature rise of approximately 0.9°C (Table 3). We can analyze the impact of increased Atlantic OHT through comparing the results of the BSO_FS_nudging

Table 3
Changes in Full-Depth-Averaged Ocean Temperature Between 2100 and 1950 for Each Region of the Arctic Ocean Based on the CTRL Experiment and CMIP6 Climate Model Simulations

	CTRL (°C)	CMIP6 MMM ± std (°C)
Arctic Ocean	1.39	1.49 ± 0.76
Central Arctic Ocean	1.30	1.30 ± 0.68
Beaufort Sea	0.90	1.09 ± 0.66
Chukchi Sea	2.23	2.27 ± 1.14
East Siberian Sea	4.00	3.34 ± 1.85
Laptev Sea	3.10	2.49 ± 1.24
Kara Sea	4.32	4.62 ± 2.37
Barents Sea	5.08	5.64 ± 2.45

Note. For CMIP6 climate model simulations, muti-model mean (MMM) ± one standard deviation (std) is given here.

experiment with CTRL experiment. Similarly, we can analyze the impact of increased Pacific OHT by analyzing the results of the BS_nudging experiment compared to the CTRL experiment, and we can investigate the combined impact of increased Atlantic and Pacific OHT by analyzing the results of the BS_BSO_FS_nudging experiment in comparison to the CTRL experiment.

We calculated contribution of the increased Atlantic and Pacific OHT to ocean warming in each region of the Arctic Ocean. First, we calculated the future change between the period 2081–2100 and the period 1950–1969 in the CTRL experiment. Second, we calculated the difference between the CTRL experiment and the nudging experiments for the period 2081–2100. Finally, by dividing the results from the second step by those from the first step, we can determine the relative contribution of the OHT in the gateways that are nudged in the corresponding experiment. Figure 3 and Table 4 show that the impacts of increased Atlantic OHT on Arctic Ocean warming will be much greater than those associated with Pacific Water. The projected warming in each Arctic region in the BSO_FS_nudging experiment is much smaller than that in the CTRL experiment (Figure 3). This suggests that increased Atlantic OHT would have notable impact on the entire Arctic Ocean, indicating that the impact of the Atlantification will extend throughout the entire Arctic

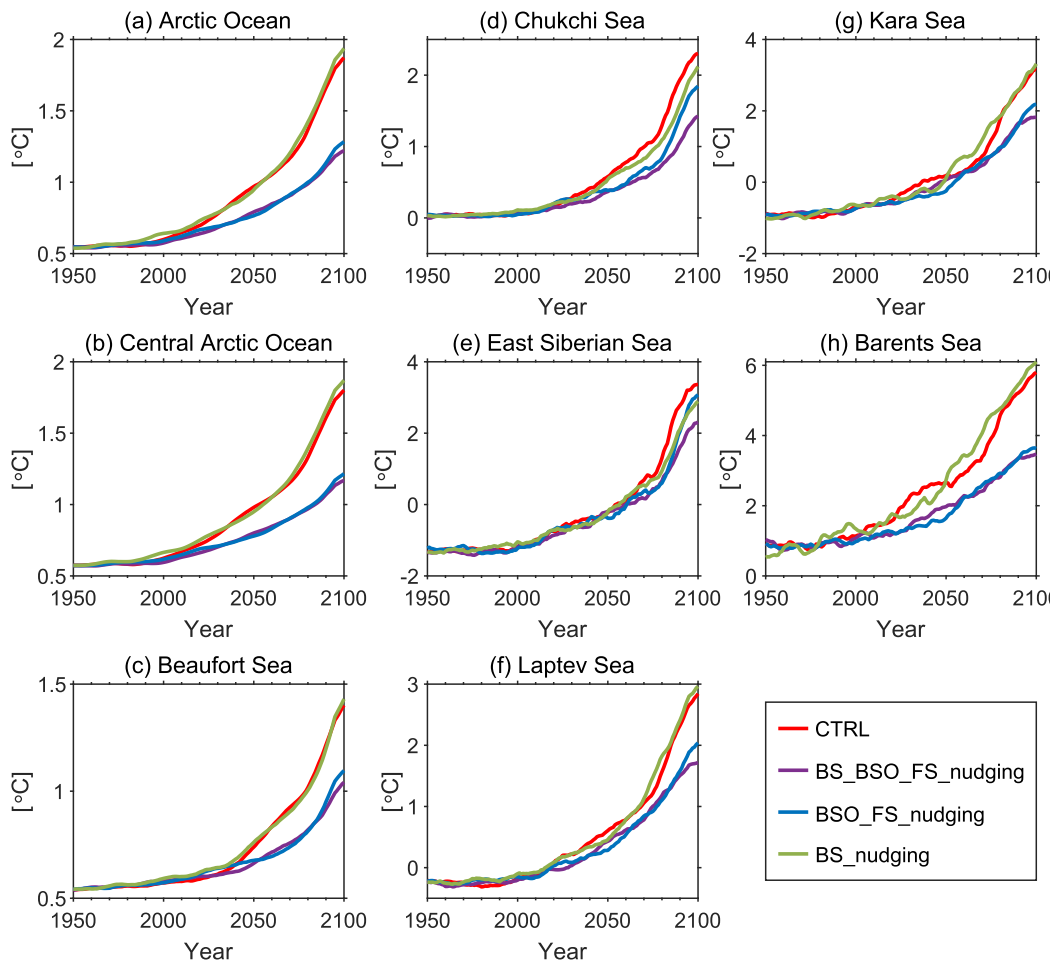

Figure 3. 11-year smoothed time series of full-depth-averaged ocean temperature for each region of the Arctic Ocean based on different experiments. Red, purple, blue, and green lines represent the results from the CTRL, BS_BSO_FS_nudging, BSO_FS_nudging, and BS_nudging experiments, respectively.

Table 4
The Contributions (Unit: %) of the Increased Atlantic and Pacific OHTs to Full-Depth-Averaged Ocean Warming and SIE Decline in Each Region of the Arctic Ocean

	Atlantic and Pacific OHT		Atlantic OHT		Pacific OHT	
	Annual mean ocean temperature	March sea ice extent	Annual mean ocean temperature	March sea ice extent	Annual mean ocean temperature	March sea ice extent
Arctic Ocean	49.2	49.7	46.3	30.2	4.3	15.5
Central Arctic Ocean	51.7	58.6	49.4	35.6	5.7	12.1
Beaufort Sea	43.4	47.5	38.8	28.2	0.7	23.4
Chukchi Sea	43.9	57.1	26.8	21.5	15.5	48.0
East Siberian Sea	27.1	64.0	16.4	44.8	15.2	43.4
Laptev Sea	32.3	–	27.8	–	4.5	–
Kara Sea	29.8	66.7	27.4	59.1	1.5	10.3
Barents Sea	45.3	15.7	43.8	14.1	5.2	0.9

Ocean in a warming climate. Without the increased Atlantic OHT, the Arctic Ocean warming is approximately only half that of the warming in the CTRL experiment (Figure 3a and Table 4). In the BS_nudging experiment, ocean temperatures in the Chukchi Sea and the East Siberian Sea are projected to be lower than the results from the CTRL experiment (Figures 3d and 3e), indicating the typical regions of notable Pacification. Table 4 shows that the contribution of Atlantic OHT to the sea water temperature in the Chukchi Sea is larger than that of Pacific OHT, whereas in the East Siberian Sea, their contributions are comparable. In the BS_BSO_FS_nudging experiment, the projected ocean temperatures in the central Arctic Ocean, Beaufort Sea, the Laptev Sea, the Kara Sea, and the Barents Sea are similar to the results from the BSO_FS_nudging experiment. However, the projected ocean temperature in the Chukchi Sea and the East Siberian Sea are lower than the results from the BSO_FS_nudging experiment (Figures 3d and 3e), which is mainly attributable to eliminated increase in OHT by Pacific Water in the BS_BSO_FS_nudging experiment.

The spatial pattern of the impacts on Arctic Ocean warming at different depths during 2081–2100 is shown in Figure 4. The differences between the CTRL and BS_BSO_FS_nudging experiments (Figures 4a–4d) represent the combined impacts of increased OHT by both the Atlantic Water and the Pacific Water. Figures 4e–4h and 4i–4l present the separate impacts of increased OHT by the Atlantic Water and the Pacific Water, respectively. Figures 4a–4d show that the combined impacts would be most notable in the Chukchi Sea, the Barents Sea, and the Eurasian Basin with gradual diminishment toward the central Arctic Ocean. Figures 4e–4h indicate that Atlantification would be most striking in the Barents Sea and the Eurasian Basin, whereas Pacification would be most marked in the Chukchi Sea (Figures 4i–4l). Figure 4 also illustrates that the impacts of increased Atlantic OHT would be most notable at intermediate depths, whereas the impacts of increased Pacific OHT would be much shallower, occurring mainly in the upper 50 m.

To investigate the Atlantic and Pacific OHT impacts at different depths in each Arctic region, we considered the temperature profiles of the CTRL and sensitivity experiments in each region during 2081–2100 (Figure 5). It is evident that increased Atlantic OHT would notably affect the water columns in the Barents Sea (Figure 5h), the Kara Sea (Figure 5g), and the East Siberian Sea (Figure 5e), and upper 2000 m of the Chukchi Sea (Figure 5d), the central Arctic Ocean (Figure 5b), and the Beaufort Sea (Figure 5c). In the Laptev Sea, its impact would be confined mainly to within the upper 1200 m (Figure 5f). For the entire Arctic Ocean, its impact is expected to be greatest at the depth of approximately 500 m (Figure 5a). Increased Pacific OHT would have greatest impact on the upper waters of the Chukchi Sea and East Siberian Sea (Figures 5d and 5e). Interestingly, the temperature of CTRL is less than BS_ nudging experiment at depths of about 200–800 m (Figure 5a). This can be explained by more Atlantic OHT in BS nudging experiment (Figures 2a and 2b). Figure 5 suggests that the impacts of Atlantification would be more prominent than Pacification in the Arctic Ocean in a warming climate, except in the upper waters of the Chukchi Sea and East Siberian Sea where Pacification is expected to be more pronounced. It is logical as the Pacific Water is located much shallower compared to the Atlantic Water. We also included ± one standard deviation of ocean temperature from the CTRL experiment in the temperature profiles in Figure S1 in

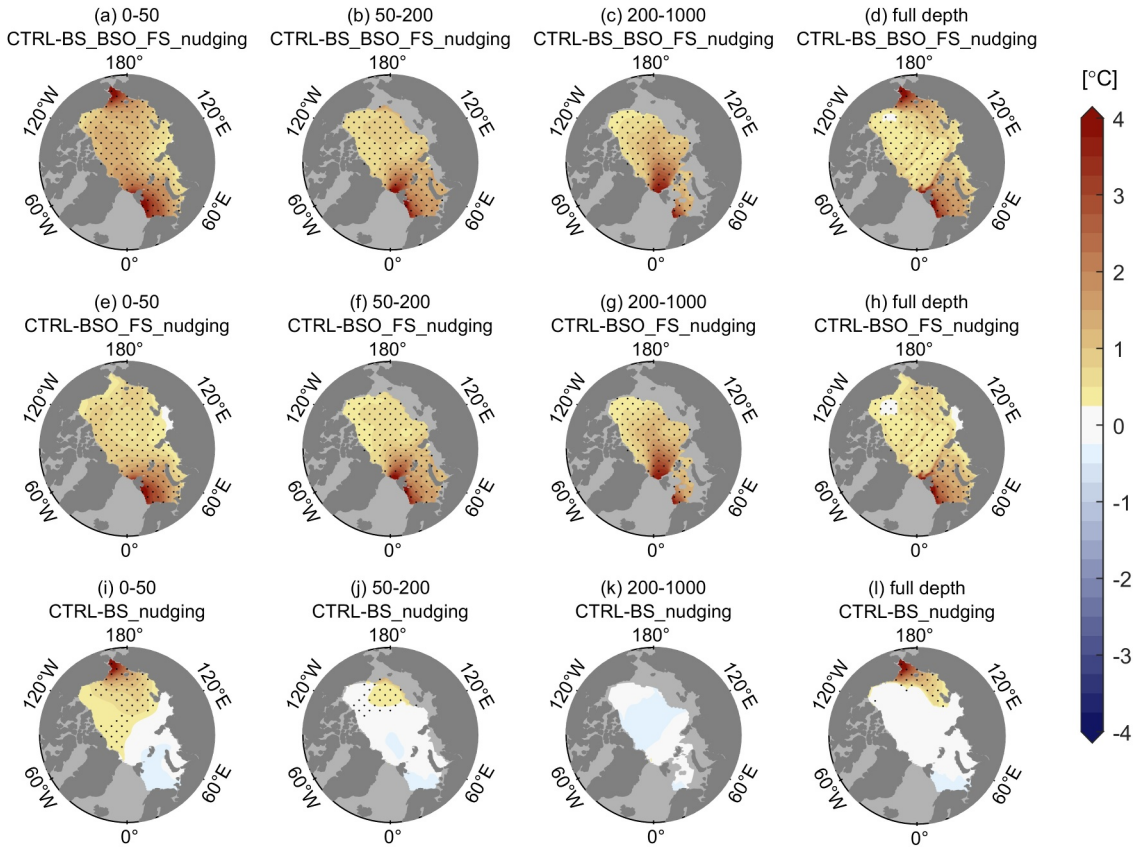

Figure 4. Temperature differences between the CTRL and sensitivity experiments in different depth ranges (0–50 m, 50–200 m, 200–1000 m, and at full depth) during 2081–2100. The black dots mark regions where the differences between the CTRL and sensitivity experiments exceed the natural variability (one standard deviation) from the CTRL experiment.

Supporting Information S1. It indicates that the impact of increased OHT on temperature changes in the sensitivity experiments is significant compared to the natural variability.

Generally, the impacts of increased Atlantic OHT in the Arctic Ocean are projected to be greater than those of increased Pacific OHT. Increased Pacific OHT would mainly affect the upper waters of the Chukchi Sea and the East Siberian Sea, whereas increased Atlantic OHT is projected to affect the entire Arctic Ocean. Without the increase in Atlantic Water temperature, the warming rate of the Arctic Ocean would be reduced by approximately half.

3.3. Impacts on Arctic Sea Ice Decline

Previous studies suggested that OHT is an important source of internal winter variability and trend of sea ice in the Arctic (Årthun et al., 2012; Dörr et al., 2021; Sandø et al., 2014; Serreze et al., 2016). To study the distinct impacts of increased Atlantic and Pacific OHT on Arctic sea ice, the simulated SIE in the four experiments in March, June, September, and December are shown in Figures 6 and S2 in Supporting Information S1.

According to the results of the CTRL experiment, the timing of notable decline of SIE varies across different Arctic regions in March, which is the representative month of the cold season (Figures 6a1–6f1). Currently, the most marked decline in winter sea ice in the Arctic Ocean is observed in the Barents Sea (Årthun et al., 2012; Onarheim et al., 2015), and our experiments indicate that increased Atlantic OHT would play a remarkable role in its future decline (Figure 6h1) consistent with previous studies (Dörr et al., 2021). Before 2050, increased Atlantic OHT is projected to contribute to the greatest reduction in cold season SIE in the Barents Sea. Increased Atlantic OHT would also influence SIE decline in other Arctic Ocean regions in the future. Without increased Atlantic OHT, the timing of cold season SIE decline would be substantially delayed in the central Arctic Ocean (Figure 6b1), the Beaufort Sea (Figure 6c1), the Chukchi Sea (Figure 6d1), the East Siberian Sea (Figure 6e1), and

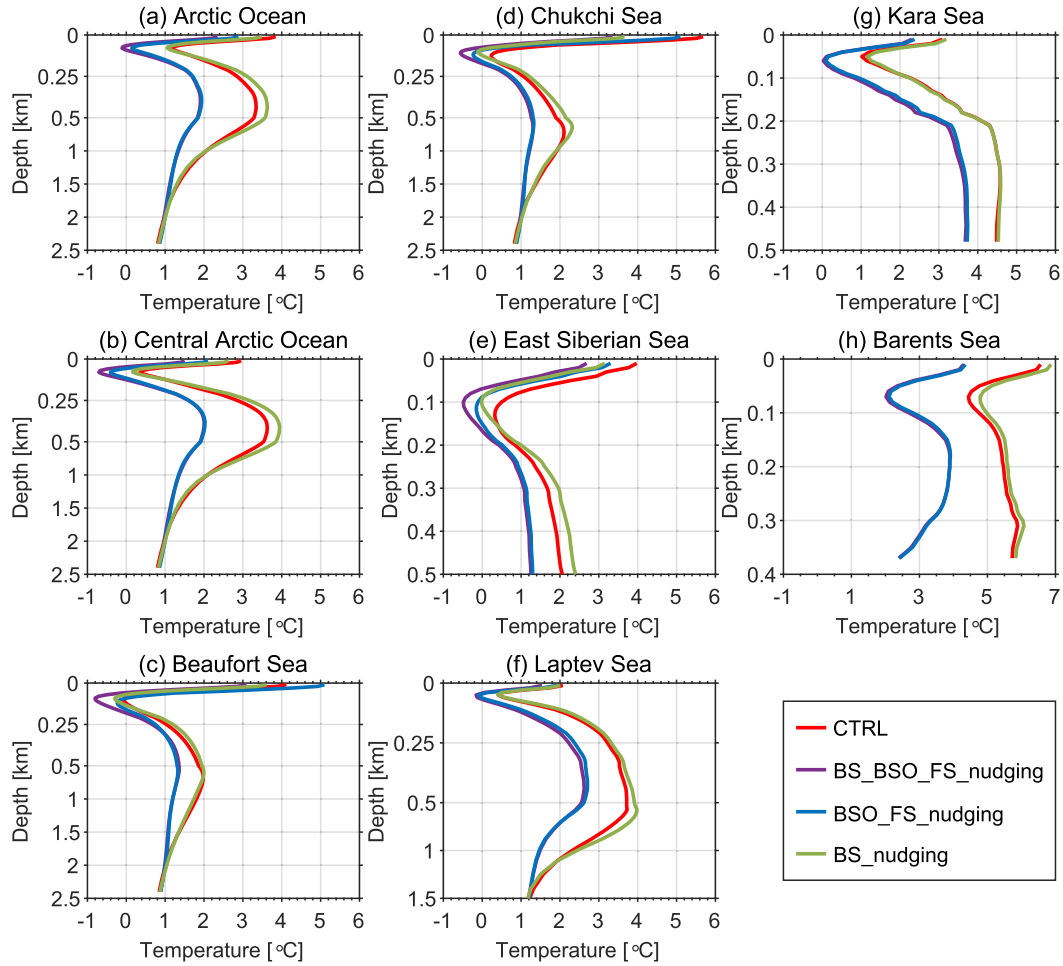

Figure 5. Temperature profile for each region of the Arctic Ocean during 2081–2100 in CTRL and sensitivity experiments. Red, purple, blue, and green lines represent the results of CTRL, BS_BSO_FS_nudging, BSO_FS_nudging, and BS_nudging experiments, respectively.

the Kara Sea (Figure 6g1), and the trends of sea ice decline in those regions would be much slower. Increased Pacific OHT is projected to primarily affect SIE decline in the Pacific sector, including the Chukchi Sea (Figure 6d1), the East Siberian Sea (Figure 6e1), and the Beaufort Sea (Figure 6c1). Its contribution is most remarkable in the Chukchi Sea, which reaches 48%. The contribution of Atlantic OHT on March SIE is most remarkable in the Kara Sea, reaching 59.1%. The impacts of Atlantic and Pacific OHT are projected to be comparable in the East Siberian Sea (more than 40%) and the Beaufort Sea (more than 20%). The Laptev Sea is expected to be covered by sea ice without impacts by either Atlantic OHT or Pacific OHT before 2100 (Figure 6f1). In other regions as well as considering the entire Arctic Ocean, the contribution of the Atlantic OHT on the decrease of March SIE is greater than that of the Pacific OHT (Table 4). September SIEs in the Barents Sea, the Kara Sea, and the Laptev Sea have been rapidly decreasing since 1950, whereas SIEs in other Arctic seas have begun to decrease rapidly since 2000, leading to the emergence of ice-free summers in the Arctic in 2040–2050 (Figures 6a2–6f2). The impacts of increased OHT on September SIE are remarkable in the Laptev Sea (Figure 6f2).

The simulated SIE in June and December are shown in Figure S2 in Supporting Information S1. June SIE in the Arctic Ocean except the Barents Sea shows a downward trend starting from 2050 (Figures S2a1–S2f1 in Supporting Information S1). The impact of Atlantic OHT on the reduction of SIE in June is greater than that of Pacific OHT in the whole Arctic Ocean including the Chukchi Sea. In December, the impact of Pacific OHT is remarkable in the Chukchi Sea during 2020–2050 (Figure S2d2 in Supporting Information S1), whereas the effect of Atlantic OHT is remarkable in the Kara Sea during 2020–2060 (Figure S2g2 in Supporting Information S1).

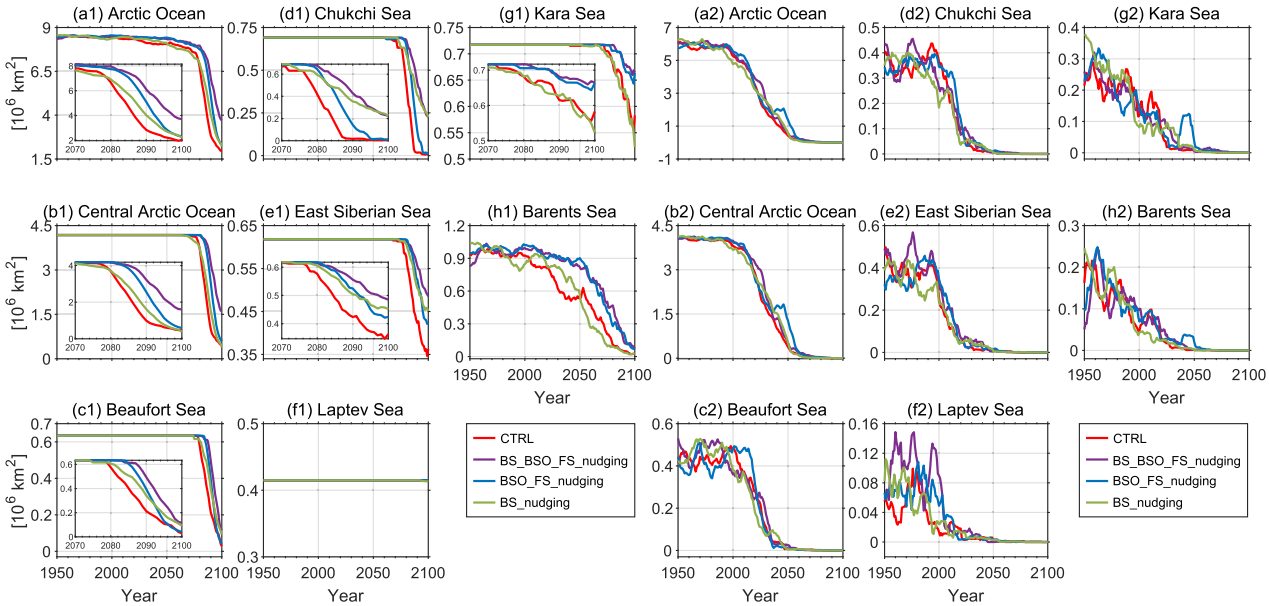

Figure 6. 11-year smoothed time series of March (a1–h1) and September (a2–h2) SIE in different regions of the Arctic Ocean. Inset panels in (a1–e1) and (g1) are the results during 2070–2100. Red, purple, blue, and green lines indicate the results of the CTRL, BS_BSO_FS_nudging, BSO_FS_nudging, and BS_nudging experiments, respectively.

The beginning time of SIE decline is delayed in the Kara Sea by approximately 20 years in the sensitivity experiments. The impacts of increased Pacific OHT and Atlantic OHT on sea ice extent in the Central Arctic Ocean, the Beaufort Sea, the East Siberian Sea, the Laptev Sea, and the Barents Sea SIE are not remarkable in December.

The projected impacts of increased Atlantic and Pacific OHT on sea ice concentration (SIC) in March, June, September, and December in the middle (2041–2060) and at the end (2081–2100) of this century are shown in Figure 7 and Figures S3–S5 in Supporting Information S1, respectively. In March, the influence of increased Atlantic OHT on SIC would be mainly evident in the northern Barents Sea, where SIC will decrease by more than 50% in the middle of the 21st century (2041–2060) (Figures 7c1 and 7f1). In the Pacific sector, the impacts of increased Pacific OHT on SIC are small (Figures 7d1 and 7g1), because the edge of sea ice in March has not retreated north of the Bering Strait, and Pacific OHT may only influence the sea ice thickness. The combined impacts on SIC would mainly reflect the contribution by increased Atlantic OHT (Figures 7b1 and 7e1). At the end of the 21st century, the influence of increased Atlantic OHT on SIC is projected to extend to the Kara Sea, the central Arctic Ocean, the Chukchi Sea, and the East Siberian Sea, causing SIC to decline (Figures 7c2 and 7f2). The central Arctic Ocean would be the area most affected. However, the impacts on the Barents Sea are projected to be small because the Barents Sea is likely to be ice-free at the end of this century (Pan et al., 2023). The increased Pacific OHT would mainly affect the Pacific sector, including the Chukchi Sea, the East Siberian Sea, and parts of the central Arctic Ocean (Figures 7d2 and 7g2), consistent with the findings of Dörr et al. (2024). The combined impacts of increased Atlantic and Pacific OHT would be most notable in the Chukchi Sea and the central Arctic Ocean (Figures 7b2 and 7e2).

In June, the increased Atlantic OHT would accelerate SIC decrease in the northern Barents Sea in the middle of the 21st century (Figures S3c1 and S3f1 in Supporting Information S1). At the end of the 21st century, the impacts of increased OHT are smaller than those in March, dominated by the increase in Atlantic OHT (Figures S3a2–S3g2 in Supporting Information S1). In September, the impacts of increased Pacific OHT on SIC are small, whereas the impacts of Atlantic OHT are mainly found in the middle of the 21st century (Figures S4a1–S4g1 in Supporting Information S1). At the end of the 21st century, the Arctic would be ice-free in September across all the experiments (Figures S4a2–S4d2 in Supporting Information S1), rendering the impacts of increased OHT to seem almost negligible (Figures S4e2–S4g2 in Supporting Information S1). In December, the increased Atlantic OHT would lead to SIC decrease in the northern Barents Sea, whereas the increased Pacific OHT will cause SIC decrease in the Chukchi Sea and part of the East Siberian Sea in the middle of the 21st century (Figures S5a1–S5g1 in Supporting Information S1). At the end of the 21st century, the Arctic will be ice-free in December in all

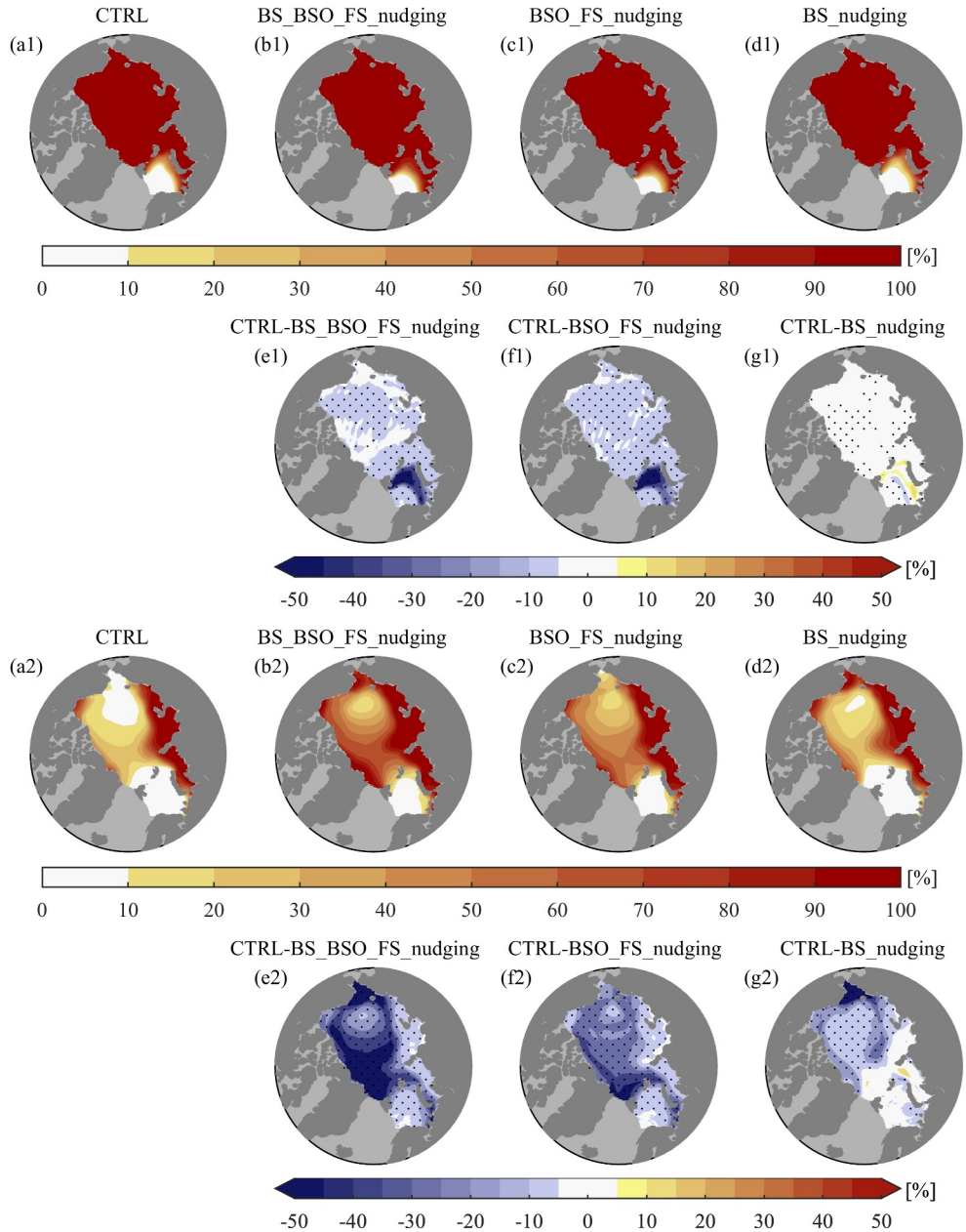

Figure 7. Simulated March sea ice concentration (a1–d1) and the differences between the CTRL experiment and the three sensitivity experiments (e1–g1) for the period 2041–2060. (a2–g2) is the same as (a1–g1) but for the period 2081–2100. The black dots mark regions where the differences between the CTRL and sensitivity experiments exceed the natural variability (one standard deviation) in the CTRL experiment.

the experiments except for the Laptev sea (Figures S5a2–S5d2 in Supporting Information S1), making the impacts of increased OHT on Arctic sea ice seem almost negligible (Figures S5e2–S5g2 in Supporting Information S1).

4. Discussion and Conclusions

In this study, we analyzed the results from three sensitivity experiments and one CTRL experiment conducted with the fully coupled FIO-ESM v2.1 to investigate the separate and combined impacts of increased Atlantic and Pacific OHT on the Arctic Ocean temperature and sea ice in a warming climate. In the sensitivity experiments, the ocean temperature was constrained to the historical climatology in the Arctic gateways to eliminate the positive trend of OHT to the Arctic Ocean. Comparison of their results with those from the CTRL experiment reveals that

Atlantification and Pacification would continue to extend toward the deep Arctic in a warming climate, and the increased OHT by both Atlantic Water and Pacific Water would contribute to Arctic Ocean warming and sea ice decline. However, the regions affected and the extent of the impacts would be markedly different.

For Arctic Ocean warming, the contribution of Atlantification will be much greater than that of Pacification. The impacts of increased Atlantic OHT will affect the entire Arctic Ocean, with the most prominent effect at intermediate depths. In contrast, the Pacific Water will mainly affect the upper Pacific sector, including the Chukchi Sea, East Siberian Sea, and Canada Basin. Without the increase in the Atlantic OHT, the rate of warming in the Arctic Ocean will decline by approximately half, but the contribution of the Pacific OHT to the overall Arctic Ocean warming will be small.

In terms of sea ice decline in the Arctic, the impacts of both Atlantic and Pacific OHT will be more notable in winter than in summer. In winter, in the first half of this century, increased Atlantic OHT will lead to sea ice decline mainly in the Barents Sea. At the end of this century, the influence of increased Atlantic OHT on SIC will extend to most of the Arctic Ocean, including the Kara Sea, central Arctic Ocean, Chukchi Sea, and East Siberian Sea, whereas increased Pacific OHT will cause sea ice decline mainly in the Pacific sector, including the Chukchi Sea, East Siberian Sea, and parts of the central Arctic area.

Our results support conclusions of previous studies, showing that enhanced OHT contributes to Arctic Ocean warming and reduction in sea ice (Docquier et al., 2021; Docquier & Koenigk, 2021; Li et al., 2017; Mahlstein & Knutti, 2011; Muilwijk et al., 2019; Pan et al., 2023; Sandø et al., 2014; Shu et al., 2021). Based on the sensitivity experiments, we further distinguished the distinct impacts of increased Atlantic and Pacific OHT on Arctic Ocean warming and sea ice decline, identifying the regions likely to be affected and the extent of their impacts.

In our sensitivity experiments, OHT through the Arctic gateways was mainly controlled by nudging the ocean temperature. This approach is similar to the restoring method employed by Docquier et al. (2021). However, unlike their method, which only restored temperature at the sea surface, we controlled the temperature across the entire depth in the gateways. Consequently, we were able to quantify more realistic impacts of increased OHT at various water depths. Another difference between this study and Docquier et al. (2021) is the external forcing applied to the climate models. Docquier et al. (2021) used constant greenhouse gas and aerosol forcing; whereas in our study, we employed the changing external forcing under the SSP5-8.5 scenario. Consequently, the results of this study should be more aligned with real-world conditions. This difference also manifests in varying relationships between changes in OHT and SIE in the two studies (Figure S6 in Supporting Information S1 and Figure 9 in Docquier et al., 2021). Figure S6 in Supporting Information S1 indicates that the relationship between changes in OHT by Atlantic Water and Arctic Ocean warming is nearly linear, but a linear relationship between changes in OHT and SIE is not clear especially when the changes in OHT are large, which is different from the results of Docquier et al. (2021). Because the impacts of increased OHT on SIE will be weakened by future global warming, such as in the Barents Sea, the differences in SIE between the four experiments will become smaller mainly due to intense surface air warming at the end of the 21st century (Figure 6h1). It must be acknowledged that OHT, as part of the coupled system, reacts to forcing, but its behavior does not entirely reflect the relationships within the fully coupled system.

Figure 2 shows that the OHT through the Fram Strait and Bering Strait can be well controlled by the nudging method. However, the OHT through the Barents Sea Opening still showed a notable positive trend in both the BS_BSO_FS_nudging experiment and the BSO_FS_nudging experiment (Figure 2a), which was mainly attributable to the increase in Atlantic Water volume transport through the Barents Sea Opening. The increased OHT in the BS_BSO_FS_nudging and BSO_FS_nudging experiments might have led to underestimated impacts of increased Atlantic OHT. Figure 2 also shows that in the BS_nudging experiment, OHT through the Barents Sea Opening is larger than that in the CTRL experiment during 2080–2100 (Figure 2a). Thus, in the BS_nudging experiment there are some warmer signals than in the CTRL experiment as shown in Figures 4 and 5. Ocean temperature nudging along the Bering Strait may lead to an increase of OHT along the Barents Sea Opening, this might be caused by the atmospheric bridge. The difference in sea level pressure between the BS_nudging and CTRL experiments indicates that in the BS_nudging experiment, there is a low-pressure difference over the Nordic Seas (Figure S7 in Supporting Information S1). The anomalous southerly winds on the eastern side of this low-pressure difference can result in warmer sea surface temperature (Figure S7 in Supporting Information S1), which then leads to an increase in OHT.

The experiments in this study were conducted under the SSP5-8.5 scenario, which represents the high-end future forcing pathway and the effects of increased OHT can be easily distinguished from the natural variability. Figures 4 and 7, S1 and S3–S5 in Supporting Information S1, suggest that the impacts of increased OHT are larger than the natural variability under the SSP5-8.5 scenario. We did not conduct experiments under low or medium emission scenarios in which the impacts of Pacific and Atlantic OHT on Arctic Ocean warming and sea ice decline are expected to be smaller than what we showed. But it should be acknowledged that additional sensitivity experiments with low- and medium-end scenarios might give additional insight.

Our experiments were conducted using a climate model with relatively low resolution. Previous studies indicate that low-resolution climate models, including those from CMIP6, exhibit common biases in simulated Atlantic Water as well as sea ice in the Arctic. Particularly, these models tend to simulate too deep and too thick Atlantic layer and underestimate the declining trend of sea ice in winter (Khosravi et al., 2022; Li et al., 2017; Pan et al., 2023; Shu et al., 2019, 2023), potentially leading to an underestimation of the impacts of increased OHT from the Atlantic Water inflow. The impacts of increased OHT on Arctic Ocean warming and sea ice decline should be investigated with high-resolution model in the future. Meanwhile, climate models exhibit significant inter-model spread, and therefore, our study based solely on one model may also have some uncertainties.

Data Availability Statement

The model data are available at https://doi.org/10.5281/zenodo.14649790 (Cheng et al., 2025).

Acknowledgments
This work was supported by the National Natural Science Foundation of China (Grants 41821004 and 42276253), Shandong Provincial Natural Science Foundation (Grant ZR2022JQ17), the Taishan Scholar Foundation of Shandong Province (Grant tsqn202211264), and Shanghai Frontiers Science Center of Polar Science (SCOPS).

References

Årthun, M., Eldevik, T., & Smedsrud, L. H. (2019). The role of Atlantic heat transport in future Arctic winter Sea Ice loss. *Journal of Climate*, *32*(11), 3327–3341. https://doi.org/10.1175/JCLI-D-18-0750.1

Årthun, M., Eldevik, T., Smedsrud, L. H., Skagseth, Ø., & Ingvaldsen, R. B. (2012). Quantifying the influence of Atlantic heat on Barents Sea Ice variability and retreat. *Journal of Climate*, *25*(13), 4736–4743. https://doi.org/10.1175/JCLI-D-11-00466.1

Bao, Y., Song, Z., & Qiao, F. (2020). FIO-ESM version 2.0: Model description and evaluation. *Journal of Geophysical Research: Oceans*, *125*(6), e2019JC016036. https://doi.org/10.1029/2019JC016036

Barton, B. I., Lenn, Y.-D., & Lique, C. (2018). Observed atlantification of the Barents Sea causes the polar front to limit the expansion of winter Sea Ice. *Journal of Physical Oceanography*, *48*(8), 1849–1866. https://doi.org/10.1175/JPO-D-18-0003.1

Boitsov, V. D., Karsakov, A. L., & Trofimov, A. G. (2012). Atlantic water temperature and climate in the Barents Sea, 2000–2009. *ICES Journal of Marine Science*, *69*(5), 833–840. https://doi.org/10.1093/icesjms/fss075

Carmack, E., Polyakov, I., Padman, L., Fer, I., Hunke, E., Hutchings, J., et al. (2015). Toward quantifying the increasing role of oceanic heat in Sea Ice loss in the New Arctic. *Bulletin of the American Meteorological Society*, *96*(12), 2079–2105. https://doi.org/10.1175/BAMS-D-13-00177.1

Cheng, K., Shu, Q., Wang, Q., Song, Z., He, Y., Wang, S., et al. (2025). Distinct impacts of increased Atlantic and Pacific Ocean Heat transport on Arctic Ocean Warming and Sea Ice decline (data) [Dataset]. *Zenodo*. https://doi.org/10.5281/zenodo.14649790

Cohen, J., Screen, J. A., Furtado, J. C., Barlow, M., Whittleston, D., Coumou, D., et al. (2014). Recent Arctic amplification and extreme mid-latitude weather. *Nature Geoscience*, *7*(9), 627–637. https://doi.org/10.1038/ngeo2234

Cohen, J., Zhang, X., Francis, J., Jung, T., Kwok, R., Overland, J., et al. (2020). Divergent consensuses on Arctic amplification influence on midlatitude severe winter weather. *Nature Climate Change*, *10*(1), 20–29. https://doi.org/10.1038/s41558-019-0662-y

Docquier, D., & Koenigk, T. (2021). A review of interactions between ocean heat transport and Arctic sea ice. *Environmental Research Letters*, *16*(12), 123002. https://doi.org/10.1088/1748-9326/ac30be

Docquier, D., Koenigk, T., Fuentes-Franco, R., Karami, M. P., & Ruprich-Robert, Y. (2021). Impact of ocean heat transport on the Arctic sea-ice decline: A model study with EC-Earth3. *Climate Dynamics*, *56*(5–6), 1407–1432. https://doi.org/10.1007/s00382-020-05540-8

Dörr, J., Årthun, M., Eldevik, T., & Madonna, E. (2021). Mechanisms of regional winter Sea-Ice variability in a warming Arctic. *Journal of Climate*, *34*(21), 8635–8653. https://doi.org/10.1175/JCLI-D-21-0149.1

Dörr, J., Årthun, M., Eldevik, T., & Sandø, A. B. (2024). Expanding influence of Atlantic and Pacific Ocean Heat transport on winter Sea-Ice variability in a warming Arctic. *Journal of Geophysical Research: Oceans*, *129*(2), e2023JC019900. https://doi.org/10.1029/2023JC019900

Duvivier, A. (2018). CICE–consortium documentation. https://buildmedia.readthedocs.org/media/pdf/cicea/latest/cicea.pdf

Eyring, V., Bony, S., Meehl, G. A., Senior, C. A., Stevens, B., Stouffer, R. J., & Taylor, K. E. (2016). Overview of the coupled model Intercomparison project phase 6 (CMIP6) experimental design and organization. *Geoscientific Model Development*, *9*(5), 1937–1958. https://doi.org/10.5194/gmd-9-1937-2016

Graversen, R. G., Mauritsen, T., Tjernström, M., Källén, E., & Svensson, G. (2008). Vertical structure of recent Arctic warming. *Nature*, *451*(7174), 53–56. https://doi.org/10.1038/nature06502

Khosravi, N., Wang, Q., Koldunov, N., Hinrichs, C., Semmler, T., Danilov, S., & Jung, T. (2022). The Arctic Ocean in CMIP6 models: Biases and projected changes in temperature and salinity. *Earth's Future*, *10*(2), e2021EF002282. https://doi.org/10.1029/2021EF002282

Lawrence, D. M., Oleson, K. W., Flanner, M. G., Thornton, P. E., Swenson, S. C., Lawrence, P. J., et al. (2011). Parameterization improvements and functional and structural advances in version 4 of the Community land model. *Journal of Advances in Modeling Earth Systems*, *3*(1). https://doi.org/10.1029/2011MS00045

Li, D., Zhang, R., & Knutson, T. R. (2017). On the discrepancy between observed and CMIP5 multi-model simulated Barents Sea winter sea ice decline. *Nature Communications*, *8*, 1–7. https://doi.org/10.1038/ncomms14991

Lien, V. S., Schlichtholz, P., Skagseth, Ø., & Vikebø, F. B. (2017). Wind-driven Atlantic water flow as a direct mode for reduced Barents Sea Ice cover. *Journal of Climate*, *30*(2), 803–812. https://doi.org/10.1175/JCLI-D-16-0025.1

Liu, J., Chen, Z., Hu, Y., Zhang, Y., Ding, Y., Cheng, X., et al. (2019). Towards reliable Arctic sea ice prediction using multivariate data assimilation. *Science Bulletin*, *64*(1), 63–72. https://doi.org/10.1016/j.scib.2018.11.018

Mahlstein, I., & Knutti, R. (2011). Ocean heat transport as a cause for model uncertainty in projected Arctic warming. *Journal of Climate*, *24*(5), 1451–1460. https://doi.org/10.1175/2010JCLI3713.1

Matishov, G., Moiseev, D., Lyubina, O., Zhichkin, A., Dzhenyuk, S., Karamushko, O., & Frolova, E. (2012). Climate and cyclic hydrobiological changes of the Barents Sea from the twentieth to twenty-first centuries. *Polar Biology*, *35*(12), 1773–1790. https://doi.org/10.1007/s00300-012-1237-9

Muilwijk, M., Ilicak, M., Cornish, S. B., Danilov, S., Gelderloos, R., Gerdes, R., et al. (2019). Arctic Ocean response to Greenland sea wind anomalies in a suite of model simulations. *Journal of Geophysical Research: Oceans*, *124*(8), 6286–6322. https://doi.org/10.1029/2019JC015101

Muilwijk, M., Nummelin, A., Heuzé, C., Polyakov, I. V., Zanowski, H., & Smedsrud, L. H. (2023). Divergence in climate model projections of future Arctic atlantification. *Journal of Climate*, *36*(6), 1727–1748. https://doi.org/10.1175/JCLI-D-22-0349.1

Neale, R. B., Gettelman, A., Park, S., Chen, C.-C., Lauritzen, P. H., Williamson, D. L., et al. (2012). Description of the NCAR community Atmosphere model (CAM 5.0). https://doi.org/10.5065/wgtk-4g06

Nguyen, A. T., Pillar, H., Ocaña, V., Bigdeli, A., Smith, T. A., & Heimbach, P. (2021). The Arctic subpolar gyre sTate estimate: Description and assessment of a data-constrained, dynamically consistent ocean-Sea Ice estimate for 2002–2017. *Journal of Advances in Modeling Earth Systems*, *13*(5), e2020MS002398. https://doi.org/10.1029/2020MS002398

Notz, D., & Stroeve, J. (2016). Observed Arctic sea-ice loss directly follows anthropogenic CO2 emission. *Science*, *354*(6313), 747–750. https://doi.org/10.1126/science.aag2345

Onarheim, I. H., Eldevik, T., Årthun, M., Ingvaldsen, R. B., & Smedsrud, L. H. (2015). Skillful prediction of Barents Sea ice cover. *Geophysical Research Letters*, *42*(13), 5364–5371. https://doi.org/10.1002/2015GL064359

Onarheim, I. H., Eldevik, T., Smedsrud, L. H., & Stroeve, J. C. (2018). Seasonal and regional manifestation of Arctic Sea Ice loss. *Journal of Climate*, *31*(12), 4917–4932. https://doi.org/10.1175/JCLI-D-17-0427.1

O'Neill, B. C., Tebaldi, C., van Vuuren, D. P., Eyring, V., Friedlingstein, P., Hurtt, G., et al. (2016). The scenario model Intercomparison project (ScenarioMIP) for CMIP6. *Geoscientific Model Development*, *9*, 3461–3482. https://doi.org/10.5194/gmd-9-3461-2016

Pan, R., Shu, Q., Song, Z., Wang, S., He, Y., & Qiao, F.-L. (2023). Simulations and projections of winter Sea Ice in the Barents Sea by CMIP6 climate models. *Advances in Atmospheric Sciences*, *40*(12), 2318–2330. https://doi.org/10.1007/s00376-023-2235-2

Polyakov, I. V., Alkire, M. B., Bluhm, B. A., Brown, K. A., Carmack, E. C., Chierici, M., et al. (2020). Borealization of the Arctic Ocean in response to anomalous advection from Sub-Arctic seas. *Frontiers in Marine Science*, *7*, 516272. https://doi.org/10.3389/fmars.2020.00491

Polyakov, I. V., Pnyushkov, A. V., Alkire, M. B., Ashik, I. M., Baumann, T. M., Carmack, E. C., et al. (2017). Greater role for Atlantic inflows on sea-ice loss in the Eurasian Basin of the Arctic Ocean. *Science*, *356*(6335), 285–291. https://doi.org/10.1126/science.aai8204

Qiao, F., Zhao, W., Yin, X., Huang, X., Liu, X., Shu, Q., et al. (2016). A highly effective global surface wave numerical simulation with ultra-high resolution. In *SC '16: Proceedings of the international conference for high performance computing, networking, storage and analysis. Presented at the SC '16: Proceedings of the international conference for high performance computing, networking, storage and analysis* (pp. 46–56). https://doi.org/10.1109/SC.2016.4

Rantanen, M., Karpechko, A. Y., Lipponen, A., Nordling, K., Hyvärinen, O., Ruosteenoja, K., et al. (2022). The Arctic has warmed nearly four times faster than the globe since 1979. *Communications Earth & Environment*, *3*, 1–10. https://doi.org/10.1038/s43247-022-00498-3

Riahi, K., van Vuuren, D. P., Kriegler, E., Edmonds, J., O'Neill, B. C., Fujimori, S., et al. (2017). The Shared Socioeconomic Pathways and their energy, land use, and greenhouse gas emissions implications: An overview. *Global Environmental Change*, *42*, 153–168. https://doi.org/10.1016/j.gloenvcha.2016.05.009

Richards, A. E., Johnson, H. L., & Lique, C. (2022). Spatial and temporal variability of Atlantic water in the Arctic from 40 Years of observations. *Journal of Geophysical Research: Oceans*, *127*(9), e2021JC018358. https://doi.org/10.1029/2021JC018358

Roach, A. T., Aagaard, K., Pease, C. H., Salo, S. A., Weingartner, T., Pavlov, V., & Kulakov, M. (1995). Direct measurements of transport and water properties through the Bering Strait. *Journal of Geophysical Research*, *100*(C9), 18443–18457. https://doi.org/10.1029/95JC01673

Sandø, A. B., Gao, Y., & Langehaug, H. R. (2014). Poleward ocean heat transports, sea ice processes, and Arctic sea ice variability in NorESM1-M simulations. *Journal of Geophysical Research: Oceans*, *119*(3), 2095–2108. https://doi.org/10.1002/2013JC009435

Sandø, A. B., Nilsen, J. E. Ø., Gao, Y., & Lohmann, K. (2010). Importance of heat transport and local air-sea heat fluxes for Barents Sea climate variability. *Journal of Geophysical Research*, *115*(C7), 2009JC005884. https://doi.org/10.1029/2009JC005884

Schauer, U., Beszczynska-Möller, A., Walczowski, W., Fahrbach, E., Piechura, J., & Hansen, E. (2008). Variation of measured heat flow through the Fram Strait between 1997 and 2006. In R. R. Dickson, J. Meincke, & P. Rhines (Eds.), *Arctic–subarctic ocean fluxes: Defining the role of the northern seas in climate* (pp. 65–85). Springer. https://doi.org/10.1007/978-1-4020-6774-7_4

Schlichtholz, P. (2019). Subsurface ocean flywheel of coupled climate variability in the Barents Sea hotspot of global warming. *Scientific Reports*, *9*, 1–16. https://doi.org/10.1038/s41598-019-49965-6

Serreze, M. C., Crawford, A. D., Stroeve, J. C., Barrett, A. P., & Woodgate, R. A. (2016). Variability, trends, and predictability of seasonal sea ice retreat and advance in the Chukchi Sea. *Journal of Geophysical Research: Oceans*, *121*(10), 7308–7325. https://doi.org/10.1002/2016JC011977

Shimada, K., Kamoshida, T., Itoh, M., Nishino, S., Carmack, E., McLaughlin, F., et al. (2006). Pacific Ocean inflow: Influence on catastrophic reduction of sea ice cover in the Arctic Ocean. *Geophysical Research Letters*, *33*(8). https://doi.org/10.1029/2005GL025624

Shu, Q., Qiao, F., Liu, J., Bao, Y., & Song, Z. (2024). Description of FIO-ESM version 2.1 and evaluation of its sea ice simulations. *Ocean Modelling*, *187*, 102308. https://doi.org/10.1016/j.ocemod.2023.102308

Shu, Q., Wang, Q., Årthun, M., Wang, S., Song, Z., Zhang, M., & Qiao, F. (2022). Arctic Ocean Amplification in a warming climate in CMIP6 models. *Science Advances*, *8*(30), eabn9755. https://doi.org/10.1126/sciadv.abn9755

Shu, Q., Wang, Q., Guo, C., Song, Z., Wang, S., He, Y., & Qiao, F. (2023). Arctic Ocean simulations in the CMIP6 ocean model Intercomparison project (OMIP). *Geoscientific Model Development*, *16*(9), 2539–2563. https://doi.org/10.5194/gmd-16-2539-2023

Shu, Q., Wang, Q., Song, Z., & Qiao, F. (2021). The poleward enhanced Arctic Ocean cooling machine in a warming climate. *Nature Communications*, *12*, 1–9. https://doi.org/10.1038/s41467-021-23321-7

Shu, Q., Wang, Q., Su, J., Li, X., & Qiao, F. (2019). Assessment of the Atlantic water layer in the Arctic Ocean in CMIP5 climate models. *Climate Dynamics*, *53*(9–10), 5279–5291. https://doi.org/10.1007/s00382-019-04870-6

Skagseth, Ø., Eldevik, T., Årthun, M., Asbjørnsen, H., Lien, V. S., & Smedsrud, L. H. (2020). Reduced efficiency of the Barents Sea cooling machine. *Nature Climate Change*, *10*(7), 661–666. https://doi.org/10.1038/s41558-020-0772-6

Skagseth, Ø., Furevik, T., Ingvaldsen, R., Loeng, H., Mork, K. A., Orvik, K. A., & Ozhigin, V. (2008). Volume and heat transports to the Arctic Ocean via the Norwegian and Barents seas. In R. R. Dickson, J. Meincke, & P. Rhines (Eds.), *Arctic–subarctic ocean fluxes* (pp. 45–64). Springer. https://doi.org/10.1007/978-1-4020-6774-7_3

Smedsrud, L. H., Esau, I., Ingvaldsen, R. B., Eldevik, T., Haugan, P. M., Li, C., et al. (2013). The role of the Barents Sea in the Arctic climate system. *Reviews of Geophysics*, *51*(3), 415–449. https://doi.org/10.1002/rog.20017

Smedsrud, L. H., Ingvaldsen, R., Nilsen, J. E. Ø., & Skagseth, Ø. (2010). Heat in the Barents Sea: Transport, storage, and surface fluxes. *Ocean Science*, *6*(1), 219–234. https://doi.org/10.5194/os-6-219-2010

Smith, R., Jones, P., Briegleb, P., Bryan, O., Danabasoglu, G., Dennis, M., et al. (2010). The Parallel Ocean Program (POP) reference manual: Ocean component of the community. *Climate System Model (CCSM)*.

Timmermans, M.-L., Proshutinsky, A., Golubeva, E., Jackson, J. M., Krishfield, R., McCall, M., et al. (2014). Mechanisms of Pacific summer water variability in the Arctic's Central Canada basin. *Journal of Geophysical Research: Oceans*, *119*(11), 7523–7548. https://doi.org/10.1002/2014JC010273

Uotila, P., Goosse, H., Haines, K., Chevallier, M., Barthélemy, A., Bricaud, C., et al. (2019). An assessment of ten ocean reanalyses in the polar regions. *Climate Dynamics*, *52*(3–4), 1613–1650. https://doi.org/10.1007/s00382-018-4242-z

Wang, M., & Overland, J. E. (2012). A sea ice free summer Arctic within 30 years: An update from CMIP5 models. *Geophysical Research Letters*, *39*(18). https://doi.org/10.1029/2012GL052868

Wang, Q., Shu, Q., Wang, S., Beszczynska-Moeller, A., Danilov, S., Steur, L., et al. (2023). A review of Arctic–Subarctic ocean linkages: Past changes, mechanisms, and future projections. *Ocean-Land-Atmosphere Research*, *2*, 0013. https://doi.org/10.34133/olar.0013

Woodgate, R. A. (2018). Increases in the Pacific inflow to the Arctic from 1990 to 2015, and insights into seasonal trends and driving mechanisms from year-round Bering Strait mooring data. *Progress in Oceanography*, *160*, 124–154. https://doi.org/10.1016/j.pocean.2017.12.007

Woodgate, R. A., & Aagaard, K. (2005). Revising the Bering Strait freshwater flux into the Arctic Ocean. *Geophysical Research Letters*, *32*(2). https://doi.org/10.1029/2004GL021747

Woodgate, R. A., Weingartner, T., & Lindsay, R. (2010). The 2007 Bering Strait oceanic heat flux and anomalous Arctic sea-ice retreat. *Geophysical Research Letters*, *37*(1). https://doi.org/10.1029/2009GL041621

Woodgate, R. A., Weingartner, T., & Lindsay, R. (2012). Observed increases in Bering Strait oceanic fluxes from the Pacific to the Arctic from 2001 to 2011 and their impacts on the Arctic Ocean water column. *Geophysical Research Letters*, *39*(24). https://doi.org/10.1029/2012GL054092